Transition Met Chem
DOI 10.1007/s11243-014-9875-0

Diferric oxo-bridged complexes of a polydentate aminopyridyl ligand: synthesis, structure and catalytic reactivity

Ambica Kejriwal · Achintesh Narayan Biswas · Amitava Choudhury · Pinaki Bandyopadhyay

Received: 26 June 2014 / Accepted: 16 August 2014

Abstract The catalytic reactivity of a group of diferric oxo-bridged complexes (**1**–**3**) of a tetradentate ligand (bpmen = *N*,*N*′-dimethyl-*N*,*N*′-*bis*(2-pyridylmethyl)-1,2-diaminoethane) toward alkane hydroxylation has been evaluated. Among the three complexes, the μ-oxo diiron(III) complex [Fe(bpmen)(μ-O)$FeCl_3$] (**1**) has been synthesized for the first time. The complex **1** has been characterized by spectroscopic analysis and X-ray crystallography. At room temperature, the μ-oxo diiron(III) complexes **1**–**3** have been found to be useful catalysts in hydroxylation of alkanes with *m*-chloroperbenzoic acid as oxidant. [Fe(bpmen)(μ-O)$FeCl_3$] (**1**) has been found to be the most active catalyst. Moreover, the catalytic ability of the complexes in the oxidation of alcohols to ketones with hydrogen peroxide at room temperature has also been investigated.

Introduction

Nonheme diiron centers bridged by oxo (or hydroxo) and carboxylato groups have attracted a great deal of interest among bioinorganic chemists over the past two decades [1–3]. Given the high stability of the μ-oxo diiron(III) motif, it is not surprising that nature has chosen this motif as the active sites of several proteins [4–9]. The μ-oxo diiron(III) unit has been found in several nonheme enzymes, which include methane monooxygenase (MMO) [5, 6], ribonucleotide reductase (RNR) [7, 8] and fatty acid desaturases [9]. These enzymes carry out diverse biological reactions such as hydroxylation of methane (MMO), toluene (toluene-4-monooxygenase), generation of tyrosine radical (RNR) and desaturation of saturated fatty acids. This fascinating pattern of reactivity shown by the μ-oxo diiron(III) motif present in the enzymes has stimulated efforts to develop analogous in model systems to provide a chemical basis for understanding the reactivity of the metalloenzymes. Over the last two decades, several complexes with the μ-oxo diiron(III) unit have been synthesized and characterized [1, 10–16]. Depending upon the bite angle of the nitrogen-rich ligands employed, μ-oxo diferric complexes with Fe–O–Fe angles ranging from 180° to 114° have been obtained [10]. In this regard, tetradentate tripodal ligands such as TPA (TPA = *tris*(2-pyridylmethyl)amine) and linear tetradentate ligands such as bpmen (bpmen = *N*,*N*′-dimethyl-*N*,*N*′-*bis*(2-pyridylmethyl)-1,2-diaminoethane) have been explored in designing a variety of dinuclear metal complexes [1, 10, 14–17]. In particular, doubly bridged oxo/hydroxo diferric complexes based on TPA have emerged as excellent structural models for compound Q of sMMO [14]. On the other hand, μ-oxo diferric complexes based on bpmen ligand [11, 15, 16] have received much less attention in this regard. Indeed a few well-characterized complexes were reported but the investigation of their catalytic ability is only limited to the epoxidation of alkenes [31]. So far, no report on the catalytic behavior of μ-oxo diferric complexes of bpmen ligand toward hydroxylation of alkanes is

Electronic supplementary material The online version of this article (doi:10.1007/s11243-014-9875-0) contains supplementary material, which is available to authorized users.

A. Kejriwal · P. Bandyopadhyay (✉)
Department of Chemistry, University of North Bengal, Raja Rammohunpur, Siliguri 734013, India
e-mail: pbchem@rediffmail.com

A. N. Biswas
Department of Chemistry, Siliguri College, Siliguri 734001, India

A. Choudhury
Department of Chemistry, Missouri University of Science and Technology, Rolla, MO 65409-0010, USA

Published online: 05 September 2014

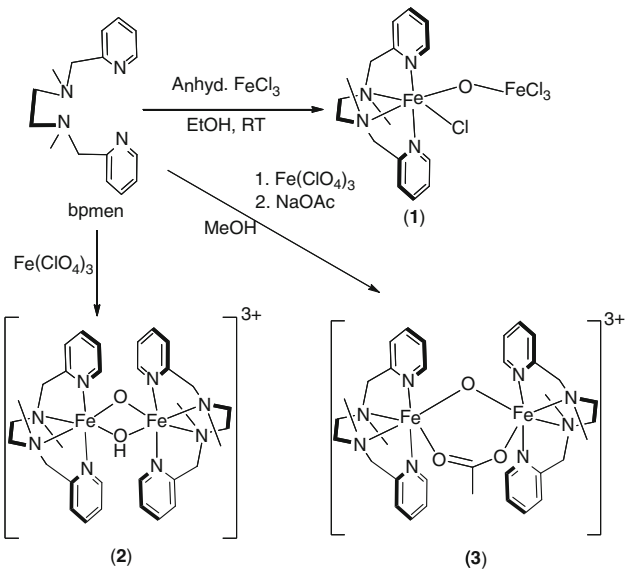

Scheme 1 Synthetic routes to complexes **1–3**

available in the literature. This prompted us to undertake a detailed study on the catalytic behavior of μ-oxo diferric complexes of bpmen ligand toward room-temperature hydroxylation of alkanes. A group of μ-oxo (**1**), (μ-oxo) (μ-hydroxo) (**2**) [15] and (μ-oxo) (μ-acetato) (**3**) [11] bridged diiron(III) complexes based on the bpmen ligand has been chosen to examine their catalytic ability toward room-temperature alkane hydroxylation with *m*-chloroperbenzoic acid. The μ-oxo diiron(III) complexes (**1–3**) differ in their coordination environment around the iron(III) centers as well as the Fe–O–Fe angles (Scheme 1). The oxo-bridged diferric complex [Fe(bpmen)(μ-O)$FeCl_3$] (**1**) has been synthesized for the first time and structurally characterized. Moreover, the catalytic efficacy of the above complexes has been further compared in oxidation of benzyl alcohols at room temperature with hydrogen peroxide.

Experimental section

Materials

All chemicals were of reagent grade and were used without further purification. The ligand *N*,*N*′-dimethyl-*N*,*N*′-*bis*(2-pyridylmethyl)-1,2-diaminoethane) (bpmen) and the diiron complexes, viz., [Fe_2(μ-O)(μ-OH)$(bpmen)_2$] (**2**) and [Fe_2(μ-O)(μ-CH_3CO)$(bpmen)_2$] (**3**) were prepared according to the published procedures [11, 15, 17]. Elemental microanalyses (C, H and N) were obtained with either a Perkin-Elmer (Model 240C) or Heraeus Carlo Erba 1108 elemental analyzer. Electronic spectra were recorded on an Agilent-5843 spectrophotometer. Gas chromatography (GC) analyses were performed on a Clarus-500 (Perkin-Elmer) GC instrument equipped with an FID detector.

Table 1 Crystallographic data and processing parameters for complex **1**

Chemical formula	C_{16} H_{22} Cl_4 Fe_2 N_4 O
Formula weight	539.88
Crystal system, space group	Monoclinic, P(2)1/c
Unit cell dimensions	
a (Å)	31.551(6)
b (Å)	10.670(2)
c (Å)	14.130(3)
α (°)	90
β (°)	102.226(3)
γ (°)	90
Volume ($Å^3$)	4648.8(16)
Z, Calculated density (mg m^{-3})	8, 1.543
Absorption coefficient (mm^{-1})	1.721
Crystal size (mm)	0.25 × 0.16 × 0.11
θ range (°) for data collection	1.98–25.00
Reflections collected/unique	44314/8190 [*R*(int) = 0.1837]
Completeness to theta = 25.00	99.9 %
Data/restraints/parameters	8190/0/491
F(000)	2192
Final *R* indices [$I > 2\sigma$ (*I*)][a, b]	*R*1 = 0.0420, w*R*2 = 0.1092
R indices (all data)	*R*1 = 0.0518, w*R*2 = 0.1130
GOF (on F^2)	1.012

[a] $R1 = (\Sigma||F_0|-|F_c||)/(\Sigma|F_0|)$

[b] $wR2 = [\Sigma w(F_0^2-F_c^2)^2/\Sigma w(F_0^2)^2]^{1/2}$

Synthesis of the complex [Fe(bpmen)(μ-O)$FeCl_3$] (**1**)

To a stirring solution in ethanol (2.0 mL) of the ligand bpmen (0.17 g, 0.629 mmol), a 2.0 mL solution of anhydrous $FeCl_3$ (0.102 g, 0.629 mmol) in 2.0 mL ethanol was added. After the addition, immediate precipitation of brown solid was observed. The precipitate was filtered off and washed with diethyl ether (Yield 0.152 g, 45 %). Anal.Calc. C, 34.54; H, 4.33; N, 10.02. Found C, 34.58; H, 4.37; N, 10.32 %. λ_{max}/nm (ε/M^{-1} cm^{-1}) = 269 (25,850), 339 (12,170), 400 (2,580).

X-ray crystallography

Single crystals of **1** were grown by slow diffusion of diethyl ether into an acetonitrile solution of the complex. Selected crystal data and data collection parameters are given in Table 1. Data on the crystals were collected on a Bruker SMART 1000 CCD area-detector diffractometer

using graphite monochromated MoKα ($\lambda = 0.71073$ Å) radiation by ω scan. The structure was solved by direct methods using SHELXS-97 [18] and difference Fourier syntheses and refined with the SHELXL97 package incorporated in WinGX 1.64 crystallographic collective package [19]. All the hydrogen positions for the compound were initially located in the difference Fourier map, and for the final refinement, the hydrogen atoms were placed geometrically and held in the riding mode. The last cycles of refinement included atomic positions for all the atoms, anisotropic thermal parameters for all nonhydrogen atoms and isotropic thermal parameters for all the hydrogen atoms. Full-matrix-least-squares structure refinement against $|F^2|$. Molecular geometry calculations were performed with PLATON [20], and molecular graphics were prepared using ORTEP-3 [21].

CCDC-989145 contains the supplementary crystallographic data for this paper. These data can be obtained free of charge from The Cambridge Crystallographic Data Centre via www.ccdc.cam.ac.uk/data_request/cif.

Catalytic reactions

Homogeneous catalytic oxidation reactions were carried out in small screw-capped vials fitted with PTFE septa. In a typical reaction, 0.7 mM concentration of catalyst and 700 mM concentration of substrate were taken in 2 mL of acetonitrile. The oxidation reaction was initiated by adding H_2O_2 (final concentration: 7.0 mM), and the contents were stirred using a magnetic bar. A standard solution of iodopentaflurobenzene was added to the reaction mixture as internal standard, and an aliquot was injected into a preheated GC. The identification and the quantization of the products were done from the response factors of standard product samples as usual. In the case of oxidation with *m*-CPBA, an acetonitrile solution (1.0 mL) of this oxidant (70 mM) was added to an acetonitrile solution (1.0 mL) of catalyst (0.7 mM) and alkane (700 mM) under nitrogen atmosphere with vigorous stirring. After 1 h, the iodopentaflurobenzene was added to the reaction mixture as an internal standard and directly analyzed by GC. In the case adamantane, CH_3CN–CH_2Cl_2 (2:3, v/v) was used as the solvent due to the poor solubility of adamantane in acetonitrile.

Results and discussion

Synthesis and characterization

The synthetic procedures for the μ-oxo diiron(III) complexes (**1**–**3**) have been outlined in Scheme 1. Reaction of equimolar amounts of bpmen and anhydrous $FeCl_3$ in ethanol under aerobic conditions afforded the μ-oxo diiron(III) complex **1**. The other two complexes (**2** and **3**) have been synthesized following a procedure already reported in the literature [11]. All the complexes have been characterized by elemental analysis and ESIMS studies. Moreover, the solid state structure of complex **1** has been confirmed by single-crystal X-ray diffraction. The molecular structure of the complex **1** is shown in Fig. 1. The crystal structure of **1** reveals two chemically identical complexes with almost identical geometries per asymmetric unit. The differic complex is comprised of two iron atoms with nonequivalent coordination spheres, in which Fe1 is six-coordinated in a pseudo-octahedral environment and Fe2 is tetra-coordinated. The two iron atoms are bridged by the oxo donor. Two pyridyl nitrogen atoms (N1 and N4), the two nitrogen atoms from the tertiary amines of the ligand bpmen (N2 and N3) and a chloride ligand constitute the coordination sphere of Fe1. In contrast, Fe2 is coordinated to the oxo donor and three chlorides. The presence of a linear μ-oxo diiron(III) unit in Complex **1** is reflected by the Fe–O–Fe bond angle of 171.21(15)° with an Fe–Fe distance of 3.531 Å, which is considerably longer than that obtained for the (μ-oxo) (μ-hydroxo)diiron(III) complex (**2**) (Table 2) [17]. The Fe–μ-O bond lengths in **1** are typical of such bonds reported in the literature (1.788(2) and 1.752(2) Å, respectively). As expected, the Fe–N_{py} bond lengths (average 2.17 Å) are shorter than the Fe–N_{amine} distances (average 2.26 Å).

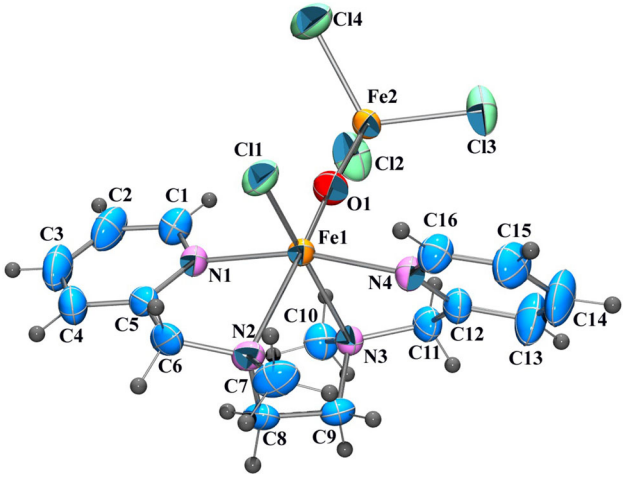

Fig. 1 Ortep plot of the complex **1** [Fe(bpmen)(μ-O)$FeCl_3$] showing 50 % probability ellipsoids

The visible range electronic spectra of complexes **1**, **2** and (μ-oxo) (μ-acetato)diiron(III) complex (**3**) in acetonitrile at room temperature are shown in Fig. 2. The spectral absorptions of μ-oxo diiron(III) complexes have been shown to be dependent on their Fe–O–Fe angles. Complexes containing a linear Fe–O–Fe unit normally show

Table 2 Selected bond lengths (Å) and bond angles (°) for the complexes **1–3**

	1[a]	**2**[b]	**3**[c]
Bond lengths (Å)			
Fe(1)…Fe(2)	3.531 (4)	2.8212 (19)	3.253 (1)
Fe(1)–μ-O(1)	1.784 (2)	1.884 (4)	1.804 (3)
Fe(2)–μ-O(1)	1.755 (2)	1.892 (4)	1.804 (3)
Fe(1)–N(1)	2.145 (2)	2.115 (5)	2.156 (6)
Fe(1)–N(4)	2.159 (2)	2.124 (5)	2.143 (6)
Fe(1)–N(2)	2.277 (3)	2.215 (5)	2.205 (6)
Fe(1)–N(3)	2.239 (3)	2.226 (5)	2.260 (6)
Bond angles (°)			
Fe1–(μ-O1)-Fe2	171.21 (15)	96.68 (19)	128.7 (4)

[a] Each asymmetric unit contains two independent molecules

[b] Ref. [15]

[c] Ref. [17]

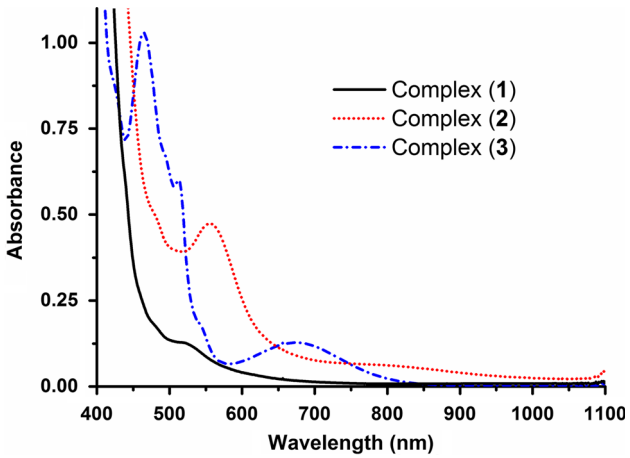

Fig. 2 UV–Vis spectra of the complexes (**1–3**) in acetonitrile at room temperature (concentration of the complexes = 1.0 mM)

bands in the 600–700 nm region and are assignable to oxo-to-iron(III) charge transfer transitions. As the Fe–O–Fe angles decrease, such bands shift toward lower wavelengths [22]. Moreover, the intensities of bands in the 400–550 nm regions increase when the Fe–O–Fe angles become more and more acute. This trend is well maintained in the symmetrical diiron(III) complexes **2** and **3**. However, no absorption corresponding to oxo-to-iron(III) charge transfer is obtained in the case of complex **1**, which can be attributed to the asymmetric coordination environment around the two iron(III) centers. The UV–Vis spectrum of complex **1** (ESI, Fig. S1) in acetonitrile exhibits an intense feature at 250 nm, which is assigned to a pyridyl π–π^* transition. Moreover, it shows characteristic bands at 339 and 400 nm, assignable to the transitions arising from ligand to metal charge transfer.

Catalytic performance of μ-oxo diiron(III) complexes

Hydroxylation of alkanes

The catalytic efficacy of the μ-oxo diiron(III) complexes (**1–3**) has been evaluated toward activation of unactivated C–H bonds, such as those in cycloalkanes. Given the higher bond dissociation energies of cycloalkanes (99.3 kcal/mol for cyclohexane), activation of C(sp^3)–H bonds is extremely challenging [23, 24]. The performance of the complexes in alkane hydroxylation at room temperature with *m*-CPBA as the oxidant has been compiled in Table 3. As evident from Table 3, the unsymmetric μ-oxo diiron(III) complex **1** emerges as a modest catalyst in alkane hydroxylation at room temperature. With a catalyst: oxidant: substrate molar ratio of 1:100:1000, the oxidation of cyclohexane has been found to be completed within an hour. Catalytic work-up and GC analysis showed the generation of cyclohexanol and cyclohexanone as the oxidation products. Conversion around 22 % was observed with a higher selectivity for the alcohol product ($A/K = 3.4$). Under identical reaction conditions, complex **3** has shown similar activity in cyclohexane oxidation affording 21 % oxygenates ($A/K = 3.0$) in 1 h. In contrast, complex **2** has been found to be a much less reactive in cyclohexane oxidation (Entry 2, Table 3). Similar results are obtained in case of cyclooctane oxidation. It is interesting to note that complex (**2**) was found to be a much superior catalyst to complex (**3**) in olefin epoxidation [31]. In order to gain further insight, the reaction of complex **2** with *m*-CPBA in presence of cyclohexane has been monitored by UV–Vis spectroscopy. Addition of *m*-CPBA to the reaction mixture containing complex **2** (1.0 mM) and cyclohexane in acetonitrile leads to the appearance of a band around 615 nm. Identical spectral changes have been observed in the absence of substrate. The observation is indicative of the formation of the salicylate bound iron(III) complex formed via *ortho*-hydroxylation of *m*-CPBA akin to what observed in reactions of mononuclear nonheme iron(II) complexes with *m*-CPBA [25]. Indeed, after acetylation of the bluish green reaction mixture with acetic anhydride and 1-methyl imidazole [25], GC analysis confirms the presence of 3-chlorosalicylic acid (0.4 TN) in the present case. Thus, catalytic hydroxylation and *ortho*-hydroxylation of *m*-CPBA have been found to be competitive in this case, which in turn justifies the lower catalytic efficiency of **2** in alkane hydroxylation.

The catalytic property of the complexes has also been studied in the oxidation of adamantane (Entry 3, Table 3). The catalytic activity of the diiron(III) complexes toward oxidation of adamantane follows the trend **1** > **3** > **2**. In the case of catalyst **1**, adamantane has been found to get oxidized to a mixture of 1-adamantanol (25 %), 2-adamantanol

Table 3 Oxidation of alkanes by *m*-CPBA catalyzed by complexes **1**, **2** and **3** at room temperature

Entry	Substrate	Catalyst	Products (% yield)[a]	*A*/*K*	3°/2°
1	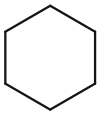	**1**	Cyclohexanol (17)	3.4	–
			Cyclohexanone (05)		
2		**2**	Cyclohexanol (09)	3.0	–
			Cyclohexanone (03)		
3		**3**	Cyclohexanol (17)	4.3	–
			Cyclohexanone (04)		
4	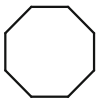	**1**	Cyclooctanol (25)	3.5	–
			Cyclooctanone (07)		
5		**2**	Cyclooctanol (11)	2.75	–
			Cyclooctanone (04)		
6		**3**	Cyclooctanol (20)	3.3	–
			Cyclooctanone (06)		
7	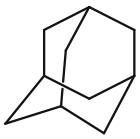	**1**	Adamantan-1-ol (25)	–	12.5
			Adamantan-2-ol (02)		
			Adamantan-2-one (04)		
8		**2**	Adamantan-1-ol (12)	–	12.0
			Adamantan-2-ol (02)		
			Adamantan-2-one (01)		
9		**3**	Adamantan-1-ol (22)	–	13.2
			Adamantan-2-ol (03)		
			Adamantan-2-one (02)		

Reaction condition: 0.7 mM catalyst, 700 mM substrate, 70 mM *m*-CPBA in acetonitrile (in case of adamantane, 2:3 acetonitrile/dichloromethane, v/v was used as solvent) at room temperature

[a] Yields are reported with respect to the initial concentration of the oxidant

(02 %) and 2-adamantanone (04 %). The normalized 3°/2° ratio in this case has been found to be 12.5. It is noteworthy that an average 3°/2° value of 2.7 has been reported in 'gif type' oxidation of adamantane, [26]. In contrast, hydroxyl radical mediated oxidation of adamantane typically yields 3°/2° values close to 2.0 [27]. The normalized 3°/2° values obtained in the present study are close to that obtained for a structurally similar μ-oxo diiron(III) complex $[Fe_2O(bipy)_4(H_2O)_2](ClO_4)_4$ [28]. The normalized 3°/2° ratios for the Fe(II)TPA $(CH_3CN)_2/H_2O_2$ system and PhIO catalyzed P450 mimics are 15–33 [29] and 11–48 [30], respectively. The enhanced regioselectivity with this catalyst using *m*-CPBA indicates the involvement of a metal-centered oxidant as an active intermediate in the oxidation of the C–H bonds of adamantane.

The exact mechanism for alkane hydroxylation with *m*-CPBA by the μ-oxo diiron(III) motifs is not completely clear to us. However, the sequence shown in Scheme 2 seems probable. We propose that addition of *m*-CPBA to the diferric complexes generates a benzoylperoxodiiron(III) species, $[Fe_2O(L)_2(OOCOC_6H_4Cl)]^{3+}$. This putative species can undergo either O–O bond homolysis or heterolysis leading to the formation of high-valent iron(IV)-oxo or iron(V)-oxo species, which in turn oxidizes the substrate. The formation of high-valent oxoiron

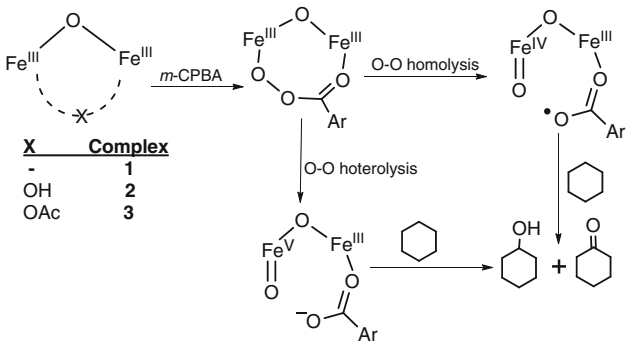

Scheme 2 Plausible mechanism for alkane hydroxylation by the μ-oxo diiron(III)complexes (**1–3**) and *m*-CPBA

transient in the present case is also consistent with high *A*/*K* ratio during cycloalkane oxidation and moderately high 3°/2° ratio during oxidation of adamantane.

Oxidation of alcohols

The reactivity of the μ-oxo diiron(III) cores toward alkanes with *m*-CPBA encouraged us to use mild and environmentally benign hydrogen peroxide as the oxidant. Akimova et al. [31] have previously studied catalytic olefin epoxidation by the complexes **2** and **3** with H_2O_2. Complex **3** has been found to be catalytically inactive while complex **2** afforded epoxides and trace amount of *cis*-diols. Therefore, in order to evaluate their ability toward catalytic hydroxylation, we attempted reactions of cycloalkanes with H_2O_2 in the presence of complexes (**1–3**). But apart from complex **2**, the other two complexes turn out to be inactive as <1 % conversion of H_2O_2 into products has been obtained. However, the μ-oxo diiron(III) complexes have been found to catalyze oxidation of alcohols at room temperature with hydrogen peroxide. Their catalytic performance has been compared using benzyl alcohol as the substrate. Interestingly, complex **1** has been found to promote oxidation of benzyl alcohol with significantly higher yield than **2** or **3** (Table 4). While the catalytic performance of complex **3**, the so called 'thermodynamic sink' [32] is not surprising, somewhat lesser yield observed in the oxidation of benzyl alcohol to benzaldehyde catalyzed by complex **2** with H_2O_2 is unusual. However, when this reaction is followed by UV–Vis spectroscopy, formation of a band at 615 nm is observed and the solution turns blue-green (Fig. 3). The spectroscopic feature is indicative of the formation of an iron(III) complex bearing a 2-hydroxy benzyl alcohol ligand derived from the aromatic ring hydroxylation of benzyl alcohol at the *ortho*-position (Scheme 3). Similar changes in electronic spectra have previously been observed in reactions between the non-heme iron(II) complex $[Fe^{II}(bqen)]^{2+}$ (bquen = *N*,*N*′-dimethyl-*N*,*N*′-*bis*(8-quinolyl)ethane-1,2-diamine) and

Table 4 Oxidation of alcohols to carbonyl compounds by hydrogen peroxide catalyzed by complexes **1, 2** and **3** at room temperature

Entry	Substrate	Catalyst	Products (% yield)[a]
1	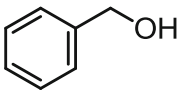	**1**	Benzaldehyde (90)
2		**2**	Benzaldehyde (65)
3		**3**	Benzaldehyde (60)
4	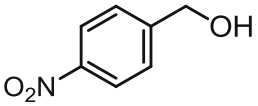	**1**	4-Nitro benzaldehyde (80)
5		**2**	4-Nitro benzaldehyde (100)
6		**3**	4-Nitro benzaldehyde (75)
7	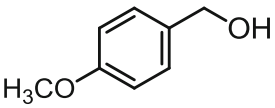	**1**	4-Methoxy benzaldehyde (70)
8		**2**	4-Methoxy benzaldehyde (60)
9		**3**	4-Methoxy benzaldehyde (50)

Reaction condition: 0.7 mM catalyst, 700 mM substrate, 7 mM H_2O_2 in acetonitrile at room temperature

[a] Yields are reported with respect to the initial concentration of the oxidant

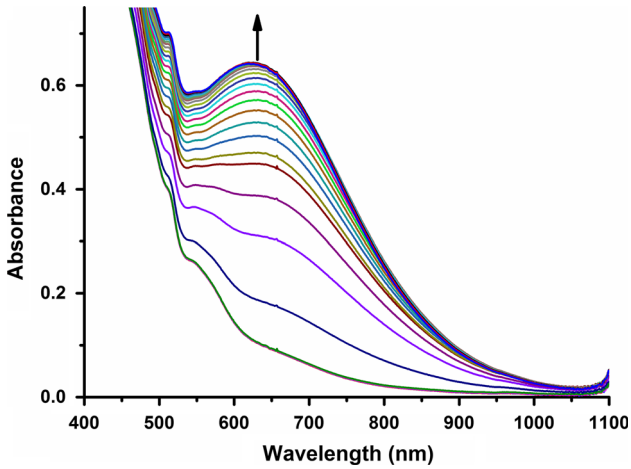

Fig. 3 UV–Vis spectral changes in the reaction of 1.0 mM [$Fe_2(\mu$-O)(μ-OH)(bpmen)$_2$] (**2**) and H_2O_2 (10 mM) in presence of 100 mM benzyl alcohol in acetonitrile at 298 K

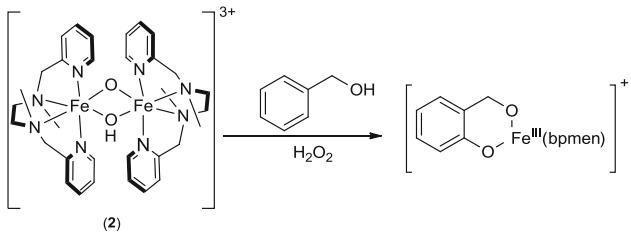

Scheme 3 *Ortho*-hydroxylation of benzyl alcohol by **2**/H_2O_2

benzyl alcohol with peracetic acid [33]. Complete absence of such iron(III) species in case of complexes **1** and **3** suggests that only complex **2** is capable of hydroxylating the aromatic ring of benzyl alcohol. This is further supported by the fact that no aromatic hydroxylation is observed for 4-nitro benzyl alcohol with **2**/H_2O_2 and the corresponding benzaldehyde is obtained quantitatively.

Conclusion

The Catalytic activity of a group of μ-oxo-bridged diferric complexes of the bpmen ligand (**1**–**3**) differing in the Fe–O–Fe angles and the coordination environment around iron(III) toward alkane hydroxylation has been studied. For the first time, it has been demonstrated that diferric oxo-bridged complexes of the bpmen ligand can catalyze the hydroxylation of alkanes at room temperature using *m*-CPBA. Among the three diferric complexes, complex **1** is hitherto unknown. The complex (**1**) featuring a linear μ-oxo bridge was characterized by single-crystal X-ray crystallography. Inert alkanes such as cyclohexane (BDE = 99 kcal/mol) and cyclooctane (BDE = 96 kcal/mol) have been oxidized to the corresponding hydroxyalkanes with moderate selectivity (A/K = 3.0–3.5). The Catalytic reactivity of complex **1** in alkane hydroxylation has been found to be greater than the other two μ-oxo diiron(III) complexes (**2** and **3**). The diiron(III) complexes (**1**–**3**) are also effective in catalytic alcohol oxidation with environmentally benign H_2O_2 as the oxidant at room temperature. The catalytic activity of the diiron(III) complexes toward oxidation of benzylic alcohols follows the trend **1** > **3** > **2**. The results clearly demonstrate the catalytic potential of suitable μ-oxo diiron(III) complexes toward oxyfunctionalization of hydrocarbons under mild condition. Further studies aimed at developing practical and synthetically useful catalytic systems based on oxo-bridged diiron(III) complexes are in progress in our laboratory.

Acknowledgments The financial support from SERB (SR/S1/IC-53/2010), DST, Government of India and CSIR (1/2498/11/EMR-II),

New Delhi, is gratefully acknowledged. We thank CSIR (India) for the award of fellowship to AK.

References

1. Que L Jr, Tolman WB (2002) Angew Chem Int Ed 41:1114
2. Kurtz DM Jr (1990) Chem Rev 90:585
3. Tshuva EJ, Lippard SJ (2004) Chem Rev 104:987
4. Wallar BJ, Lipscomb JD (1996) Chem Rev 96:2625
5. Merkx M, Kopp DA, Sazinsky MH, Blazyk JL, Müller J, Lippard SJ (2001) Angew Chem Int Ed 40:2782
6. Rosenzweig AC, Fredrick CA, Lippard SJ, Nordlund P (1993) Nature 366:537
7. Jordan A, Reichard P (1998) Annu Rev Biochem 67:71
8. Logan DT, Su XD, Åberg A, Regnström K, Hajdu J, Eklund H, Nordlund P (1996) Structure 4:1053
9. Broadwater JA, Ai J, Loehr TM, Sanders-Loehr J, Fox BG (1998) Biochemistry 37:14664
10. Norman RE, Holz RC, Ménage S, O'Conor CJ, Zhang JH, Que L Jr (1990) Inorg Chem 29:4629
11. Hazell R, Jensen KB, McKenzie CJ, Toftlund H (1995) J Chem Soc Dalton Trans 5:707
12. Esmelindro MC, Oestreicher EG, Márquez-Alvarez H, Dariva C, Egues SMS, Fernandes C, Bortoluzzi AJ, Drago V, Antunes OAC (2005) J Inorg Biochem 99:2054
13. Khattar R, Hundal MS, Mathur P (2012) Inorg Chim Acta 390:129
14. Xue G, De Hont R, Münck E, Que L Jr (2010) Nat Chem 2:400
15. Taktak S, Kryatov SV, Rybak-Akimova EV (2004) Inorg Chem 43:7196
16. Duban EA, Drebushchak TN, Bryliakov KP, Talsi EP (2007) Mendeleev Commun 17:291
17. Okuno T, Ito S, Ohba S, Nishida Y (1997) J Chem Soc Dalton Trans 19:3547
18. Sheldrick GM (1997) SHELX97, University of Göttingen, Germany
19. Farrugia LJ (2003) WinGX Version 1.64, An Integrated System of Windows Programs for the Solution, Refinement and Analysis of Single-Crystal X-ray Diffraction Data, Department of Chemistry, University of Glasgow
20. Spek AL (2003) PLATON. J Appl Crystallogr 36:7
21. Farrugia LJ (1997) J Appl Crystallogr 30:565
22. Poussereau S, Blondin G, Cesario M, Guilhem J, Chottard G, Gonnet F, Girerd JJ (1998) Inorg Chem 37:3127
23. White MC (2012) Science 335:807
24. Chen MS, White MC (2010) Science 327:566
25. Makhlynets OV, Das PP, Taktak S, Margaret F, Ruben MB, Rybak-Akimova EV, Que L Jr (2009) Chem Eur J 15:13171
26. Barton DHR, Boivin J, Motherwell WB, Ozabalik N, Schwarzentruber KM, Jankowski K (1986) New J Chem 10:387
27. Singh B, Long JR, De Biani FF, Gatteschi D, Stavropoulos P (1997) J Am Chem Soc 119:7030
28. Menage S, Vincent JM, Lambeaux C, Fontecave M (1994) J Chem Soc Dalton Trans 2081
29. Kim C, Chen K, Kim J, Que L Jr (1997) J Am Chem Soc 119:5964
30. Kitajima N, Fukui H, Moro-oka Y (1988) J Chem Soc Chem Commun 7:485
31. Taktak S, Kryatov SV, Hass TE, Rybak-Akimova EV (2006) J Mol Catal A Chem 259:24
32. Norman RE, Yan S, Que L Jr, Backes G, Ling J, Loehr JS, Zhang JH, O'Connor JC (1990) J Am Chem Soc 112:1554
33. Yoon J, Wilson SA, Jang YK, Seo MS, Nehru K, Hedman B, Hodgson KO, Bill E, Solomon EI, Nam W (2009) Angew Chem Int Ed 48:1257